ELSEVIER

Nuclear Instruments and Methods in Physics Research A 464 (2001) 433–439

NUCLEAR INSTRUMENTS & METHODS IN PHYSICS RESEARCH Section A

www.elsevier.nl/locate/nima

A 3.3 MJ, Rb^{+1} driver design based on an integrated systems analysis☆

Wayne R. Meier[a,*], John J. Barnard[a], Roger O. Bangerter[b]

[a] *Lawrence Livermore National Laboratory, P.O. Box 808, L-446, Livermore, CA 94551, USA*
[b] *E.O. Lawrence Berkeley National Laboratory, Berkeley, CA 94720, USA*

Abstract

A computer model for systems analysis of heavy ion drivers has been developed and used to evaluate driver designs for inertial fusion energy. The present work examines a driver for a close-coupled target design that requires less total beam energy but also smaller beam spots sizes than previous target designs. Design parameters and a cost estimate for a 160 beam, 3.3 MJ driver using rubidium ions ($A = 85$) are reported, and the sensitivity of the results to variations in selected design parameters is given

Keywords: Fusion; Heavy Ion; Inertial fusion; Driver; Accelerator; Systems model

1. Introduction

Ion Beams for Energy Applications Model (IBEAM) is an integrated source-to-target computer model for induction linac drivers for inertial fusion nergy (IFE) that includes the key interdependencies of the major subsystems in terms of cost, performance and constraints [1]. We are using this model to investigate design options for drivers for IFE power plants. Our objectives are to find minimum cost configurations that meet specified target requirements and to identify factors that have the highest leverage for cost reduction. Previous systems modeling and conceptual design studies for HIF drivers can be found in Refs. [2–6].

At the previous Symposium on Heavy Ion Inertial Fusion, we described a 5.9 MJ driver design that used heavy ions ($A \sim 200$) [7]. In this paper, we focus on a driver for the close-coupled target design that requires less total energy but also smaller beam spot size on target (1.7 mm vs. 2.7 mm). We also use a much lighter ion, rubidium ($A = 85$), in order to reduce the driver cost. Table 1 lists the requirements for the close-coupled target. The foot and main pulse ion energies in Table 1 are less than those reported in Refs. [8,9] by the ratio of ion masses (85/207) in order to keep the ion range in the radiators approximately constant.

The models in IBEAM are, for the most part, based on current technologies with assumptions for technology improvements and component cost reductions that might be possible by the time a driver is built. The US HIF program is currently working on component cost reduction for key

☆This work was performed under the auspices of the U.S. Department of Energy by the University of California, Lawrence Livermore National Laboratory under Contract No. W-7405-Eng-48.

*Corresponding author. Tel.: +1-925-422-8536; fax: +1-925-422-7390.

E-mail address: meier5@llnl.gov (W.R. Meier).

0168-9002/01/$ - see front matter
PII: S0168-9002(01)00101-2

Table 1
Close-coupled target requirements

	Foot pulse	Main pulse
Ion mass (amu)	85	
Final ion energy (GeV)	0.90	1.44
Beam energy (MJ)	0.50	2.80
Total charge (mC)	0.55	1.95
Pulse duration on target (ns)	30	8
Spot radius on target (mm)	1.7	

items such as ferromagnetic core material, pulsed-power subsystems, insulators and quadrupole magnets. Some of the models, e.g., the final focusing algorithms, are based on early work in the field. Beam transport through the chamber and final focus is now receiving significant attention in the US, and better models will be developed and incorporated into IBEAM in due course. In addition, entirely new technologies or significant advances are possible; e.g., we have not yet considered the impact of using high temperature superconductors on the design and cost. Despite these limitations, interesting and useful conclusions can be drawn from IBEAM.

2. Design description

2.1. Overview

The driver consists of a multibeam injector, an acceleration section to bring the beams to the final energy required by the target, a final transport section used to compress the beams to the final pulse duration and redirect the beams for two-sided illumination of the target, and the final focus magnet set. Magnetic focusing is used throughout the accelerator; there is no electrostatic section at the low energy end as in the previous design [7]. (The cost advantage of an electrostatic front end was found to be small, with transition to magnetic focusing becoming cost effective at an ion energy of $\sim$3 MeV without beam merging and 4 MeV with merging.) The basic design approach is to distribute the 2.5 mC of charge (determined by the total megajoules on target and final ion energies for the foot and main pulses) into many parallel beams. The design described here has a total of 160 beams. This array of beams and associated quadrupole magnets pass through common induction cores in a re-entrant configuration. By using a large number of small beams, the current though the induction cores is increased leading to high driver efficiency ($\sim$42% for the base case). The scaling for magnetic focusing is also favorable in that as the number of beams increases the radial build of the array decreases, and this reduces the total mass of ferromagnetic material needed to provide the required acceleration.

Of the 160 beams, 36 provide the 0.8 MJ foot pulse and 124 provide the 2.5 MJ main pulse. In the initial part of the accelerator all beams are identical and are transported in a single array. Once the ions reach the foot pulse energy (0.9 GeV), the array is divided into two parallel arrays; the 118 main pulse beams continue acceleration up to 1.44 GeV, while the foot beams are simply transported without further acceleration. At the point where the main pulse beams reach their final energy, both arrays are split in half and redirected for two-sided illumination of the target. Depending on the ion parameters, the total length of the final transport section is either set by the required length for drift compression or the length needed to redirect the ion path through the bends (depends on ion rigidity and bending magnet strength—assumed to be 4 T in this case). The final transport length is 230 m for this design.

2.2. Acceleration schedule

The beams are injected into the main accelerator with initial ion energy of 2.0 MeV and pulse duration of 15 μs, giving an average current per beam of 1.04 A and a bunch length of 32 m. The source radius per beam is 5.9 cm. The beam radius is compressed in the injector/matching section and enters the accelerator with an average radius of 2.0 cm.

The initial acceleration gradient depends on the initial bunch length (and thus pulse duration) since we assume the maximum velocity tilt is 0.3. This lead to a maximum acceleration gradient of 0.6 of the initial ion energy divided by the initial bunch

length. For the base case design, this is an initial acceleration gradient of $(0.6 \times 2.0\,\mathrm{MeV})/(32\,\mathrm{m}) = 37.5\,\mathrm{kV/m}$. The acceleration gradient increases linearly with ion energy subject to a limit on the core radial build of 1 m, which corresponds to $\sim 1.5\,\mathrm{V\,s/m}$ for the assumed flux swing of 2.3 T and core material radial and axial packing fractions of 80%. The acceleration gradient continues to increase up to a maximum of 2.0 MV/m.

2.3. Beam variations versus ion energy

Fig. 1 summarizes the variation of key beam parameters with increasing ion energy. All values are normalized to the initial beam parameters except the current, which is normalized to the final beam current of 78 A. As indicated, the beam current rises rapidly from the initial 1.04 A as the pulse duration decreases as discussed below.

The pulse duration decreases rapidly (from $\tau_0 = 15\,\mu\mathrm{s}$) as a result of increasing ion velocity and decreasing bunch length. In this example, we limit the pulse duration to a minimum of 200 ns. (If the beam pulse becomes too short, the rise and fall times of the voltage pulse consumes a significant part of the core volt-seconds, which does not contribute to beam energy, thus reducing the accelerator efficiency.) Initially, the bunch length decreases as $1/T_i^{1/2}$. Because of the limitation on pulse duration, the bunch length actually passes through a minimum of 5.2 m at $T_i = 150\,\mathrm{MeV}$ and then increases to keep τ constant, reaching a final length of 9.1 m for the foot pulse beams and 11.3 m for the main pulse beams. In the drift compression region, the foot pulse beams are further compressed to 30 ns (1.35 m) while the main pulse beams are compressed to 8 ns (0.45 m).

As the ion energy increases, magnetic focusing of the beam is more efficient for a given field gradient. We therefore compress the beams radially with increasing ion energy until the ions reach T_{FIX}, beyond which the beam radius is fixed. This reduces the radial build of the quad array and thus the mass of core material (see Fig. 2). In our example case, $T_{FIX} = 0.5\,\mathrm{GeV}$, at which point the average beam radius is 0.77 cm. Once the beam

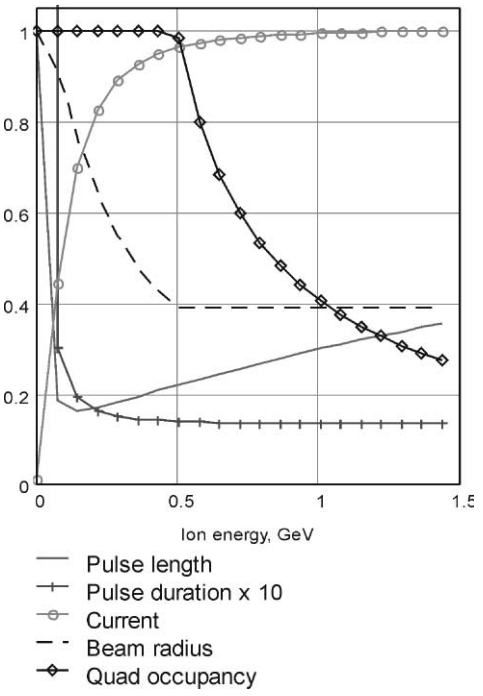

Fig. 1. Variation of beam parameters with ion energy normalized to: pulse length = 32 m, pulse duration = 15 μs, current = 78 A, beam radius = 2.0 cm, quad occupancy = 75%.

radius is fixed, the quad occupancy fraction can be reduced with increasing ion energy as shown in Fig. 1. Note that the quad occupancy fraction decreases from 75% initially to 20.5% at the end of the accelerator (for the main pulse).

The inner radius of the induction cores is an important parameter that affects the driver cost since it determines the mass of ferromagnetic material needed. Fig. 2 shows the core inner radius as a function of ion energy. It decreases with increasing ion energy as the beam radius is reduced (see Fig. 1). At $T_i = 0.5\,\mathrm{GeV}$, the beam radius is fixed preventing further decrease in core radius. Limiting the beam radius is done on the expectation that beyond some point there will be diminishing returns (or increased costs) with further reduction. At $T_i = 0.9\,\mathrm{GeV}$, the 36 foot-pulse beams are split off, and the array of main pulse beams is smaller, thus the drop in core radius.

The calculated spot size on target (1.7 mm in this case) depends on several assumptions. First we

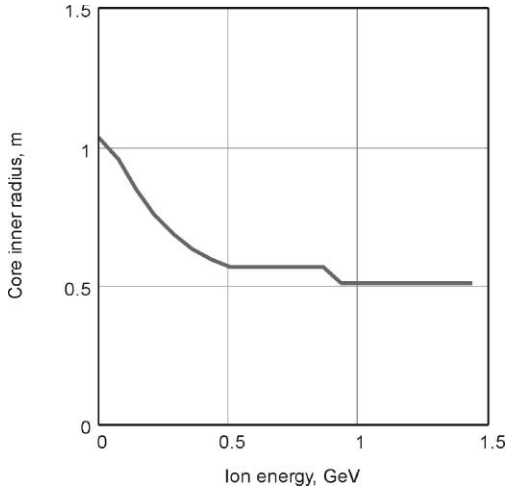

Fig. 2. Core inner radius versus ion energy.

assume neutralized ballistic focusing with 99% beam neutralization. The final focus length is 5.5 m consistent with the HYLIFE-II chamber design. The source radius of 5.9 cm (which depends on the number of beams), an estimated source temperature of 0.1 eV, and an assumed emittance growth of 2.5 × in the injector/matching section give a transverse normalized emittance of 0.33 mm mrad at the beginning of the accelerator. We assumed additional 3 × growth in normalized emittance in the accelerator for a final transverse emittance of 1 mm mrad at the final focus magnets. (Adding an emittance growth model is a planned improvement for IBEAM.) The final longitudinal emittance is 4.6 × the initial longitudinal emittance. An aiming contribution to spot size of 200 μm is included based on the design criteria for the target injector. When the space charge, emittance, chromatic aberrations, geometric aberrations and aiming contributions are added in quadrature, we find that the focusing half angle that minimizes the spot size is 6 mrad. Thus, the average beam radius at the last focus magnet is 3.3 cm.

2.4. Summary of key design parameters

Table 2 summaries important driver parameters at key points along the accelerator: at injection, at the foot pulse energy, and at the main pulse energy. Also shown are the parameters after compression to the final pulse duration.

Table 2
Summary of key parameters for reference case

Number of beams (Foot/Main/Total)			36/124/160
Initial pulse duration (μs)			15
End beam radial compression (MeV)			500
Accelerator quadrupole field at winding (T)			3.5
Final transport quad field at winding (T)			3.0
Final focus length (m)			5.5
Beam focus half angle (mrad)			6
	Along accelerator		
	Injector exit	Foot pulse	Main pulse
Ion energy (GeV)	0.002	0.90	1.44
Pulse duration (μs)	20	0.20	0.20
Beta	0.007	0.15	0.19
Pulse length (m)	32.0	9.1	11.3
Beam current (A)	1.0	77	78
Beam radius (cm)	1.96	0.77	0.77
Bore radius (cm)	3.66	1.73	1.73
Winding radius (cm)	4.52	2.40	2.40
Field gradient (T/m)	78	146	146
Core inner radius (m)	1.02	0.57	0.51
Core build (m)	0.40	0.91	0.91
Quad Occupancy (%)	75	45	20.5
Half lattice period (m)	0.23	1.02	1.45
Accel. gradient (MV/m)	0.038	2.0	2.0
Dist. from injector (km)	0	0.64	0.91
	At last final focus quadrupole		
	Foot pulse		Main pulse
Pulse duration (μs)	30		8
Pulse length (m)	1.35		0.45
Beam current (kA)	0.52		1.95
Beam radius (cm)	3.3		3.3
Bore radius (cm)	5.9		5.9
ε_n (mm mrad)	1.0		1.0
Focus half-angle (mrad)	6		6

3. Cost estimate

Table 3 shows a level-2 cost breakdown for the 3.3 MJ, Rb^{+1} design. The total driver equipment subtotal is $477 M. The injector, at $47 M, is about 10% of the driver equipment cost. The quad transport components and accelerator modules are the dominant cost items at 29% and

Table 3
Cost breakdown for 3.3 MJ, Rb^{+1} driver

Subsystem	Direct cost, ($M)		
1. Injector			47
2. Magnetic focus section			363
2.1 Quad transport		137	
Magnets	70		
Cyrostats	32		
Refrigeration	36		
2.2 Accelerator modules		157	
Metglas	81		
Structures	49		
Insulators	27		
2.3 Accel. power supplies		32	
Pulsers (switches)	17		
Storage and PFN	15		
2.4 Vacuum systems		37	
3. Final transport			65
3.1 Quad magnetic		6	
3.2 Dipole magnetic		17	
3.3 Cryostat		12	
3.4 Refrigeration		17	
3.5 Vacuum system		14	
4. Final focus magnets			2
Driver equipment subtotal			477
Allowance for I&C			57
Allowance for installation			160
Total direct cost			694

33% of the driver equipment cost, respectively. Power system costs and the vacuum system for the accelerator add a combined 14%. The final transport section accounts for 14%, and the final focus magnets are less than 1% of the equipment cost. Instrumentation & Controls (I&C) are calculated as 12% of the driver equipment cost and Assembly and Installation is taken as 30% of the sum of driver equipment and I&C, combining to add ~46%. The total direct cost is $0.69B or ~$210/J of beam energy. The total capital cost for the driver would typically be a factor of two greater than this direct cost.

4. Sensitivity to key design variables

In selecting the reference case design we examined variations with key design variables including the initial pulse duration, τ_0, the number of beams, N_b, and the quad field at the winding, B_w. Some design features that depend on these are discussed below.

4.1. Initial pulse duration

As previously noted, the initial acceleration gradient increases with decreasing pulse duration, and this results in a shorter accelerator and somewhat less core material. Fig. 3 shows the mass of core material per meter as a function of ion energy for different τ_0. The shorter τ_0, the higher the kg/m early in the accelerator (due to the higher gradient), but the overall accelerator length is shorter. The net effect is a slight reduction in the total mass of core material with decreasing τ_0. The total ferromagnetic material mass and accelerator lengths for these three cases are given in Table 4. The shorter τ_0, however, requires higher source current (higher cost injector) giving a larger beam radius at the source and larger initial emittance.

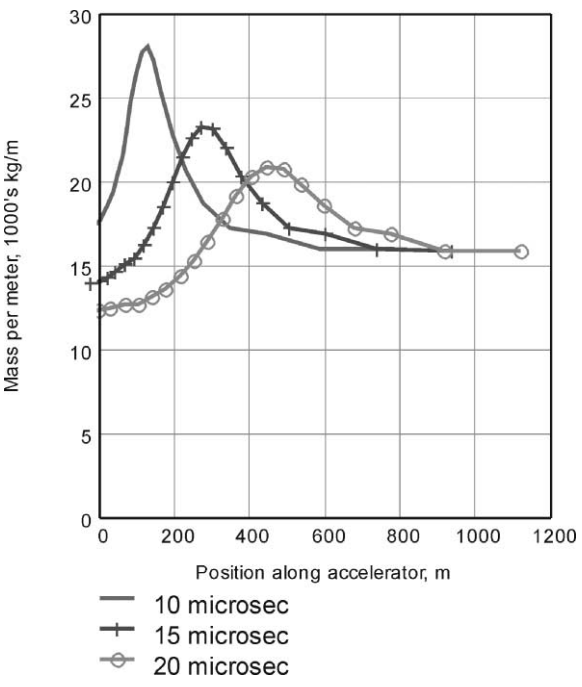

Fig. 3. Mass of ferromagnetic material per unit length (1000's kg/m) along the accelerator for different initial pulse durations.

Table 4
Variation in total mass of ferromagnetic material and accelerator length with initial pulse duration

Initial pulse duration (μs)	Core mass (10^6 kg)	Accelerator length (km)
10	15.5	0.83
15	16.1	0.91
20	16.7	1.00

Thus, if the pulse is too short, the spot size on target may be too large. On the other hand, if τ_0 is too large, the total bunch compression ratio from source to target is large, and this increases the spot size due to chromatic aberrations. The selected design point approaches a minimum driver cost while meeting spot size constraints.

4.2. Number of beams

The number of beams, N_b, is an important design parameter. As N_b increases, the total current through the common cores increases, the beam radius shrinks and the outer radius of the core decreases. At some point, the fixed clearance allowance between the beam edge and the bore reduces the attractiveness of going to a larger number of beams. Also, for use with the thick liquid wall chamber design, HYLIFE-II, the difficulty of protecting the final focus magnets with crossing jets of Flibe becomes more difficult with more beams [10,11]. As currently envisioned, each final focus magnet will require radiation shielding around the bore, which increases the magnet radial built and the overall size of the final focus array [12]. If the array is too large, the angle of the beams as they approach the target can exceed the requirements of the target design. Currently an entrance angle of $\sim 12^\circ$ is specified [8].

4.3. Quadrupole field

Another design variable is the quad field at the winding. In the IBEAM model, a single value for B_w is used for the entire accelerator, and the value of B_w that minimizes the driver cost is selected. For the reference case, we find that $B_w \sim 3.5$ T (to the nearest 0.5 T) gives the minimum cost, but the sensitivity to variations about this point is not very large. To see if varying B_w in different sections of the accelerator would make a difference, the optimum B_w was found for just the first 100 MeV of the accelerator. We found that a slightly smaller value of B_w was optimum at the low energy end, but the cost difference for the first 100 MeV was only 0.1%.

4.4. Cost sensitivity to parameter variations

Fig. 4 shows the sensitivity of the cost to a $\pm 50\%$ change in the reference case design parameters. Although continuing to decrease the beam radius (i.e., increasing T_{FIX}) would reduce the cost a couple percent, the beams would become very small indeed (down to 5 mm at 0.9 GeV and 4 mm at 1.44 GeV). The reference case, 160 beams, is optimum with a $\sim 10\%$ increase in cost for $\frac{1}{2}$ the number of beams and 4% increase for 50% more beams. A somewhat higher initial pulse duration would reduce the cost by 1%, but the spot size constraint would not be met. A 50% variation

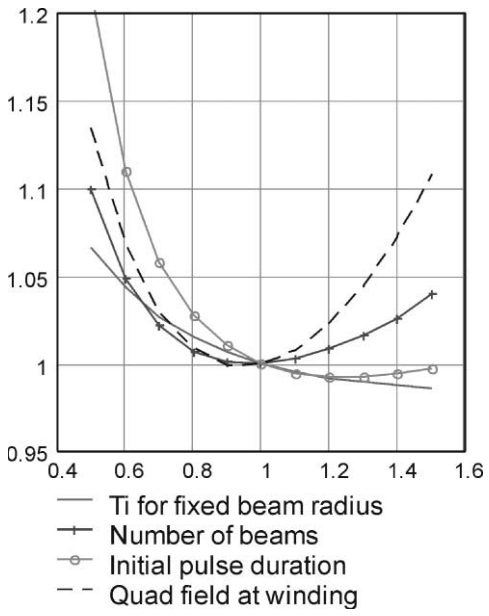

Fig. 4. Sensitivity of driver cost to variations about reference parameters: $T_{FIX} = 0.5$ GeV, $N_b = 160$, $\tau_0 = 15$ μs, $B_w = 3.5$ T.

from the 3.5 T quad field, gives about a 11–13% increase in cost.

5. Conclusions

We have developed and continue to refine a useful systems analysis tool for investigating ion driver designs for IFE. This paper has described a new point design for a 3.3 MJ close-coupled target. Although much work is needed in developing better models for many aspects of the driver (e.g., the injector costing, the final focus modeling, etc.), we have combined our best current understanding and have been able to use the code to select a design point that gives near minimum cost while meeting the constraints on beam energy and required spot size on target.

Acknowledgements

We would like to thank our colleagues in the heavy ion fusion program for their assistance, particularly Andy Faltens, Ed Lee, Joe Kwan, Grant Logan and Alex Friedman. This work was performed under the auspices of the U.S. Department of Energy by the University of California, Lawrence Livermore National Laboratory under Contract No. W-7405-Eng-48.

References

[1] W.R. Meier, LLNL Report, UCID-XXX, February, 2000.
[2] D.J. Dudziak, W.W. Saylor, W.B. Herrmannsfeldt, Fusion Technol. 13 (1988) 207.
[3] D.S. Zuckerman, D.E. Driemeyer, L.M. Waganer, D.J. Dudziak, Fusion Technol. 13 (1988) 217.
[4] J. Hovingh, V.O. Brady, A. Faltens, D. Keefe, E.P. Lee, Fusion Technol. 13 (1988) 255.
[5] R.L. Bieri, M.J. Monsler, W.R. Meier, L. Stewart, Fusion Technol. 21 (1992) 1583.
[6] J.J. Barnard et al., LLNL Report UCRL-LR-108095, September 21, 1991.
[7] W.R. Meier, R.O. Bangerter, A. Faltens, Nucl. Instr. and Meth. in Phys. A 415 (1998) 249.
[8] D.A. Callahan-Miller, M. Tabak, Nucl. Fusion 39 (1999) 1547.
[9] D.A. Callahan-Miller, M. Tabak, Progess in heavy ion fusion targets, Paper presented at the 13th. Int. Symp. on Heavy-ion Inertial Fusion, San Diego, CA, March 2000.
[10] R.W. Moir, Chamber, target and final focus integrated design, Nucl. Instr. and Meth. A 464 (2001) 140, these proceedings.
[11] P.A. House, LLNL Report, UCRL-ID-137282 Rev. 1, January 18, 2000.
[12] J.F. Latkowski, Improved final focus shielding designs for modern heavy-ion fusion power plant designs, Nucl. Instr. and Meth. A 464 (2001) 152, these proceedings.